ARTICLE

Adsorption Behavior of CH_2 and CH_3 on Metal Clusters Cu_n (n=1-6)

Xi-hui Cheng, Ming-xing Jin, Zhan Hu, Fei-fei Hu, Da-jun Ding*

Institute of Atomic and Molecular Physics, Jilin University, Changchun 130012, China

(Dated: Received on May 4, 2008; Accepted on June 12, 2008)

Using density functional theory with generalized gradient approximation and hybrid functional, we studied the properties of energy, charge population, and vibration of CH_2 and CH_3 adsorbed on Cu_n (n=1-6) clusters. The results show that the DFT calculation with the hybrid functional matches the experimental results better in both cases. The calculation results indicate that the adsorption of CH_2 is stronger than that of CH_3. During adsorption, the charges transfer from Cu to CH_2 or CH_3. The obtained vibrational frequencies for different modes of CH_2 and CH_3 adsorbed on Cu_n agree well with the experimental results for the adsorption on Cu(111) surface.

Key words: Adsorption, CH_2, CH_3, Cu cluster

I. INTRODUCTION

Adsorption of simple molecules or radicals on metal surfaces has been a subject of intensive study in recent years [1-5]. As important intermediates in a variety of addition, abstraction and insertion reactions, methyl CH_3 and methylene CH_2 have attracted wide attention from the researchers in the diverse fields of surface chemistry [6-12]. Experimentally, the studies were performed by various methods such as high resolution electron energy loss spectrometer (HREELS), X-ray photoelectron spectroscopy (XPS), Auger electron spectroscopy (AES), thermal desorption spectroscopy (TDS), and low-energy electron diffraction (LEED). Theoretically, simulation for a bulk solid surface is generally based on a cluster modeling in which a metal surface was modeled by a certain number of metal atoms nearby the adsorbate [3,4,13]. Using this modeling in density functional theory (DFT) with PW91 [14], Michaelides *et al.* investigated the softening of C−H vibrational frequencies and their implications for dehydrogenation of adsorbed hydrocarbons of CH_3 on Cu (111), Ni (111), and Pt (111), and found the fcc hollow to be favoured [15]. Robinson *et al.* performed the adsorption energy calculation of CH_3 on Cu (111) by DFT with revised Perdew, Burke, and Ernzerhof (PBE) functionals [16,17], and the calculations show a small energy difference favouring the hcp sites. They also found that the Cu−C nearest-neighbor distance is close to the experimental value and the Cu−C layer spacing is larger than the experimental value. These studies have shown that this modeling is one of the feasible ways to deal with the adsorption problem on metal surface.

In this work, we investigate the adsorption of CH_2 and CH_3 radicals on simple metal clusters Cu_n (n=1-6) theoretically by means of DFT. The adsorption behaviors, including geometries, adsorption energies, natural population analysis (NPA) charge, and vibrational frequencies, were computed.

II. CALCULATION METHODS

All the calculations of DFT methods in the present work are based on programming in GAUSSIAN 03 [18]. The methods used are the generalized gradient approximation (GGA) [19] with Perdew-Wang parameterization (PW91) [15] of the gradient corrected exchange-correlation energy and the Becke's three parameters hybrid functional (B3LYP) [20]. For hydrogen and carbon, we take the basis set of 6-311++G(3d,f). For metal copper atoms, the LANL2DZ basis set and the corresponding Los Alamos relativistic effective core potential (RECP) [21] are necessary in the calculations. The obtained adsorption energies are corrected by the counterpoise correction method to eliminate the effects of basis set superposition error (BSSE) [22,23] and the spin contamination is negligible, as described in Ref.[5]. Analysis of vibrational frequencies is performed to make sure the optimized geometries are minima, instead of transition structures.

III. RESULTS AND DISCUSSION

A. Geometry

The geometries of CH_2-Cu_n and CH_3-Cu_n are calculated and optimized by the B3LYP and PW91 methods. The geometries obtained with B3LYP method are given in Fig.1 and those from PW91 are similar with only some small differences in the structure parameters, with the exception of the adsorption of CH_2 or CH_3 on the Cu_6 cluster. The resulting geometries of Cu_6 cluster before and after adsorbing CH_2 and CH_3 are very differ-

*Author to whom correspondence should be addressed. E-mail: dajund@jlu.edu.cn

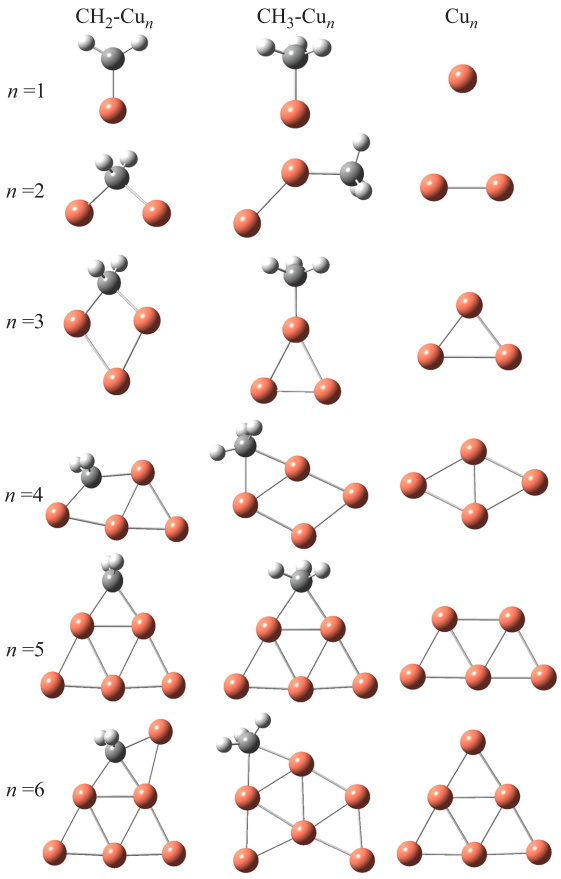

FIG. 1 Optimized structures for CH_2-Cu_n, CH_3-Cu_n, and Cu_n (n=1-6) by B3LYP method.

ent from the calculation by B3LYP method, while they are the same when using PW91 method. Although, for small n, the most stable geometries of Cu_n clusters are two-dimensional (2D) [24], all the optimizations for the adsorption of CH_2-Cu_n and CH_3-Cu_n are initially from 2D and 3D geometries as much as possible in order to avoid trapping into local minima. In all cases of n=1-6, the obtained 2D geometries are more stable than the 3D ones, similar to the bare Cu_n clusters. Here we refer to those in which the C and Cu atoms are in one plane without regarding H atoms as 2D geometries, and refer to the others as 3D geometries. This can be interpreted by the fact that a certain potential barrier needs to be overcome if the geometrical structure of the clusters undergoes a transformation from 2D to 3D during adsorbing. The geometrical structure parameters are shown in Table I.

Although there is a certain difference for C−H bond length in CH_2 and CH_3, the C−H bond lengths in these adsorption systems tend to be equal and agree with CH_3 adsorbed on Cu (111) surface [16]. The C−H bond lengths obtained from B3LYP method are smaller than those from PW91 method, but the bond lengths of Cu−Cu and Cu−C obtained from B3LYP are 0.1 Å longer than those from PW91 method. These Cu−C

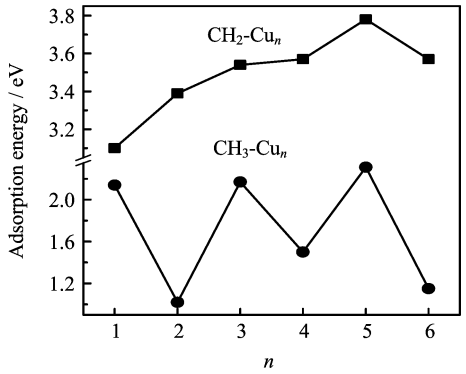

FIG. 2 Adsorption energy of CH_2 and CH_3 on Cu_n from B3LYP calculation.

bond lengths are longer than those from the CO adsorption on Cu_n calculated by Post and Baerends [25]. Thus, the present result indicates that the adsorption of CH_2 and CH_3 is weaker than that of CO on Cu_n clusters. With increasing n, the Cu−C bond length approaches gradually the experimental value of 2.22 Å measured from the adsorption on Cu (111) by Pascal *et al.* [12].

B. Adsorption energy and NPA charge analysis

The calculation of the adsorption energy is very important in a theoretical investigation of an adsorption process since the adsorption of simple molecules or radicals on solid surfaces typically involves the sequential filling of adsorption sites characterized by distinct adsorption energies. Based on the optimization structures obtained, the adsorption energies are calculated by using B3LYP and PW91 methods.

$$E_b = (E_{Cu_n} + E_{CH_x}) - E_{CH_xCu_n} \quad (1)$$

The adsorption energies obtained from B3LYP and PW91 are quite different. PW91 method leads to energies approximately 0.2-0.6 eV higher than those from B3LYP for CH_2Cu_n. PW91 method gives CH_3 adsorption energy of −0.20 eV when adsorbing on Cu. This suggests that PW91 method is not suitable in the calculation of adsorption energy for CH_3Cu_n since the adsorption energy defines a value larger than zero. Therefore, we will discuss the adsorption energy calculated from B3LYP method.

From Fig.2, one can see that, for CH_2Cu_n, the adsorption energy increases with increasing number of Cu atom for n=1-5. The adsorption energy of CH_2Cu_6 is 0.21 eV smaller than that of CH_2Cu_5, and is the same as that of CH_2Cu_4. From the geometry structures, one can see that, after adsorbing CH_2 molecule, Cu_n clusters maintain original bare cluster structures for n=1, 2, 3, and 5, but the structures are different for n=4 and 6. The calculation indicates that, in CH_2Cu_4 and

DOI:10.1088/1674-0068/21/05/445-450

TABLE I The geometry parameters of CH_2 and CH_3 molecule adsorbed on Cu_n (n=1-6) obtained by B3LYP and PW91 methods; the bond lengths of R_{C-H} and R_{Cu-Cu} shown are average values (in Å); the bond angles (in (°)) for CH_2Cu_n and CH_3Cu_n (n=4, 5, 6) are measured with C as the culmination atom, others with Cu as the culmination atom; q_{CH_2} and q_{CH_3} mean NPA charge population for CH_2 and CH_3 molecules (arbitrary units).

	B3LYP					PW91				
CH_2Cu_n	R_{Cu-C}	R_{C-H}	R_{Cu-Cu}	$\angle\alpha$	q_{CH_2}	R_{Cu-C}	R_{C-H}	R_{Cu-Cu}	$\angle\alpha$	q_{CH_2}
n=1	1.867	1.088			−0.5856	1.846	1.095			−0.4660
n=2	1.898	1.091	2.780	98.2	−0.9172	1.882	1.098	2.718	92.5	−0.8691
	1.898					1.882				
n=3	1.928	1.092	2.560	90.8	−0.8898	1.919	1.100	2.511	87.1	−0.8574
	1.929					1.919				
n=4	1.982	1.100	2.419	139.4	−0.9553	1.902	1.104	2.478	86.9	−0.8243
	2.113					1.962				
n=5	2.014	1.094	2.451	74.9	−0.6906	1.982	1.101	2.433	75.8	−0.7013
	2.014					1.981				
n=6	1.972	1.099	2.449	76.0	−1.1041	1.970	1.103	2.446	51.2	−1.0583
	2.040			73.3		2.046			51.1	
	B3LYP					PW91				
CH_3Cu_n	R_{Cu-C}	R_{C-H}	R_{Cu-Cu}	$\angle\alpha$	q_{CH_3}	R_{Cu-C}	R_{C-H}	R_{Cu-Cu}	$\angle\alpha$	q_{CH_3}
n=1	1.923	1.091			−0.4010	1.905	1.098			−0.3779
n=2	1.960	1.091	2.354	133.4	−0.3617	1.945	1.098	2.331	134.6	−0.3550
n=3	1.960	1.094	2.425	151.5	−0.5400	1.947	1.107	2.401	156.2	−0.5092
				153.6					148.6	
n=4	2.114	1.097	2.428	66.9	−0.6189	2.098	1.105	2.408	67.2	−0.5855
	2.171					2.150				
n=5	2.114	1.098	2.432	68.9	−0.6329	2.106	1.106	2.411	68.9	−0.6004
	2.133					2.106				
n=6	2.111	1.098	2.453	68.8	−0.6210	2.152	1.105	2.439	67.7	−0.5641
	2.138					2.096				
Cu(111)	2.22+0.02 [12]	1.089[a]								
$-CH_3$	1.99[a]	1.088[a]								
	1.98[a]									

[a] C−Cu bond length is layer spacing [16].

CH_2Cu_6, CH_2 has taken the position where a Cu atom was in the original bare cluster. For this change of the cluster structures a potential barrier needs to be overcome, resulting in the decreasing of adsorption energy; thus there is a drop of adsorption energy in CH_2-Cu_n (n=4, 6). The adsorption energy of CH_2 on Cu_n (n=1-6) is in the range of 3.10 eV to 3.78 eV. Compared with the adsorption energies on various surfaces listed in Table II, they are lower than those from DFT calculations by Psofogiannakis *et al.* for Pt_{10} [26] and by Oudenhuijzen *et al.* for Pt_4/F_2O and Pt_4/Na_2O [27], but similar to that for diamond [28]. Therefore, the adsorption of CH_2 on Cu_n (n=1-6) cluster is weaker than on Pt_n (n=10, 4) clusters.

The adsorption energy of CH_3 on metal surface is always lower than that of CH_2 on metal surface, as well as on Cu_n (n=1-6) clusters. The adsorption energies of CH_3 on Cu_n (n=1-6) exhibit odd/even alternation in which the energies with an odd number of Cu atoms are larger than those with an even number, suggesting easier adsorbing of CH_3 with an odd number of Cu atom clusters. Compared with CH_3 adsorption on other surfaces listed in Table II, the adsorption energies of CH_3 on Cu_n (n=1-6) are lower than that for CH_3 on diamond (100) and (111) calculated by different methods [28-30]. These values are also lower that that for CH_3 on Pt_4/F_2O and Pt_4/Na_2O [27]. But the calculated values for CH_3 on Pt_{10} cluster (2.17 eV) [26] and on Cu(111) [15,16] are in the even-odd alternative range of CH_3 on Cu_n (n=1-6) clusters. It can be concluded that the adsorption capacity of CH_3 is weaker than that of CH_2 adsorbed on Cu_n clusters, which is consistent with the adsorption energy order CH_3<CH_2<CH obtained by Povedal *et al.* of CH_n (n=1, 2, 3) adsorption on Ni(100) [4].

NPA can give some information of whether the charge

DOI:10.1088/1674-0068/21/05/445-450

TABLE II The calculation adsorption energies of CH_2 and CH_3 radicals on Cu_n (n=1-6) clusters compared with the previous results for several metal surfaces (in eV).

	CH_2	CH_3
Cu_n (n=1-6)	3.10-3.78	1.02-1.15 (even), 2.14-2.31 (odd)
Cu(111)		1.35 (top) [15], 1.866 (H-bridge) [16], 1.892 (H-top) [16], 1.47 (bridge) [15]
Diamond(100)	4.68(one fold) [28], 3.54 (bridge) [28]	3.36 [28]
Diamond(111)	3.76 [28]	2.68 [28], 4.50 [29], 3.58 [30]
Pt(111)	4.21 (bridge) [26]	2.17 (top) [26], 2.05 (top) [15]
Pt_4/F_2O	5.74 (top) [27]	3.15 [27]
Pt_4/Na_2O	5.47 (top) [27]	3.31 [27]
Ni(100)	1.96 [4]	1.23 [4]

TABLE III Vibrational frequencies of C−H in CH_2Cu_n (n=1-6) clusters obtained by B3LYP method (in cm^{-1}).

Species	ρ_{CH_2}	δ	ν_s	ν_{as}
CH_2-Cu	590.47592	1278.48904	2963.85237	3073.04598
CH_2-Cu_2	710.91579	1264.78948	2938.95067	3025.85277
CH_2-Cu_3	663.3237	1231.85268	2922.4119	3025.6105
CH_2-Cu_4	726.52988	1280.02353	2899.96408	2978.50209
CH_2-Cu_5	573.35233	1320.95081	2924.82396	2995.07336
CH_2-Cu_6	789.43948	1298.86073	2869.49433	2935.33639
Cu(111) [8]	798	1032-1379	2850	2960
CH_2/Ru(001) [34]	890	1065-1295	2870	2945
$=CH_2$ [35]	775	1440-1480	2850	2925

transfer exists in the adsorption process [31,32]. We calculate the NPA charge, instead of Mulliken population, for CH_2 and CH_3, because the Mulliken population analyses depend strongly on the basis set used and the results may be influenced by the chosen polarization and diffuse functions in the calculation. Since the 6-311++G(3d,f) basis set used in the calculation involves these functions, the NPA charge analysis is more appropriate than the Mulliken population analysis [5]. The change tendency of NPA charge obtained by two methods is the same in CH_2 and CH_3 adsorptions and the charge populations obtained by B3LYP method are generally larger than that by PW91 method. For CH_2Cu_n, q_{CH_2} increases monotonically with increasing Cu atom, except for n=5 in which q_{CH_2} is smaller than that of neighboring clusters. For CH_3Cu_n, q_{CH_3} with n=2 and 6 is smaller than their neighboring clusters. Generally, q_{CH_2} is larger than q_{CH_3}, indicating the charge transferred from metal cluster to CH_2 is more than that to CH_3. In particular, in the case of Cu_6, q_{CH_2} is nearly twice as large as q_{CH_3} for CH_3 adsorbing. Together with the adsorption energy, one can see that the more charge transferred, the bigger the adsorption energy. It is concluded that there is more charge transferred to CH_2 than to CH_3 when they are adsorbed on Cu_n (n=1-6) clusters. This behavior of charge transfer is the same as the situation for CH_2 and CH_3 adsorbed on Ni_{14}(100) [4], namely the charge is transferred from the metal cluster to radicals.

C. Frequency analysis

For all the clusters studied above, the vibrational frequencies were calculated. All the data have been revised by a scale factor of 0.9614 [33]. In the following, we present and discuss only the results obtained by B3LYP method.

These vibrations can be identified into three classes: the vibrations of Cu atoms, the vibrations of Cu and C atom, and the vibrations of C and H atom. Among them, the interatomic vibrational frequencies of Cu are weaker and have frequencies smaller than 300 cm^{-1}, but the vibrational frequencies of C−H stretching are stronger and have frequencies larger than 2500 cm^{-1}, and the frequencies of C−H bending are between 1000 and 2500 cm^{-1}. These calculated C−H vibrational frequencies for CH_2 and CH_3 on Cu_n (n=1-6) clusters are listed in Tables III and IV. For CH_2-Cu_n (n=1-6), there are four vibrational modes listed: plane wigwagging of methylene radical (ρ_{CH_2}), C−H bending (δ), and symmetric and antisymmetric C−H stretching (ν_s, ν_{as}). The C−H vibrational frequencies of methylene on metal surfaces [8,34] and methylene radical [35] are listed in the Table III and Table IV for comparison. The vibrational frequency of plane wigwagging for CH_2 increases

DOI:10.1088/1674-0068/21/05/445-450

TABLE IV Vibrational frequencies of C−H in CH_3Cu_n (n=1-6) clusters obtained by B3LYP method (in cm^{-1}).

Species	δ_s	δ_{as}	ν_s	ν_{as}
CH_3-Cu	1070.79819	1388.02115	2915.85544	3010.33049
		1388.07163		3010.70255
CH_3-Cu_2	1016.84653	1368.63289	2911.72863	3011.9492
		1382.27842		3026.94886
CH_3-Cu_3	1069.4553	1387.47556	2891.17015	2967.29476
		1389.37317		2973.14027
CH_3-Cu_4	1129.28178	1386.57425	2856.5586	2912.70763
		1388.40331		2967.05336
CH_3-Cu_5	1144.07898	1386.3786	2847.82716	2902.641
		1394.14258		2961.98553
CH_3-Cu_6	1125.16766	1383.2479	2851.14101	2890.92807
		1386.04403		2968.86002
Cu(111) [8]	1169	1371	2790	2940
Cu(111) [36]	1435	1464	2808	2888, 2922
CH_3−Ni(111) [10]	1220	1320	2655	2730
CH_3−Pt(111) [9]	1153	1363	2839	2879
$-CH_3$ [35]	1365-1380		2870	2960
CH_3 [37]	606.453	1401.6	3004.43	3160.821

with increasing cluster size with odd/oven alternation, which is closer to that of CH_2 on Cu(111) and that of methylene radical. The vibrational frequency of symmetric and antisymmetric stretching for C−H decreases with the increasing of n, and approaches that of CH_2 adsorbed on metal surfaces [8,34]. But the vibrational frequency of scissors wigwagging for C−H is higher than that of CH_2 on metal surfaces, and lower than that of methylene radical. For CH_3-Cu_n (n=1-6), the calculation gives four vibrational modes: symmetric and antisymmetric C−H bending (δ_s, δ_{as}), symmetric and antisymmetric C−H stretching (ν_s, ν_{as}). The vibrational frequency of symmetry deformation of C−H increases with the cluster size increasing and approaches the experimental value for CH_3 on Cu(111) [8]. The vibrational frequency of antisymmetric C−H bending is also in agreement with the experimental value [8]. As for the vibrational frequencies of symmetric and antisymmetric C−H stretching for CH_3 on Cu_n (n=1-6), they decrease with increasing cluster size and also approach to the experimental value for CH_3 on Cu(111) [8]. These values are also very close to those of methyl radical [35] but are smaller than those of the stable CH_3 [37]. The theoretical calculations do not show the overtones of the symmetric and antisymmetric C−H bending modes, ($2\delta_{as}$-CH_3) 2710 cm^{-1} and ($2\delta_s$-CH_3) 2290 cm^{-1}, which were observed in experiment [8]. This situation is the same as other calculations for CH_3 on metal surfaces [9,10]. It can be explained by the fact that a Fermi resonance might take place between the overtones of symmetric or antisymmetric C−H bending mode and a C−H stretching mode, determined by the higher-order derivatives of the system energy [13]. In addition, the calculated results show two frequencies for each antisymmetric C−H bending and C−H stretching mode which are from the two types for each mode that cannot be distinguished in experiment due to the resolution.

IV. CONCLUSION

Using density functional theory with generalized gradient approximation (GGA) and hybrid functional, the adsorption properties of CH_2, CH_3 molecules on Cu_n (n=1-6) clusters are studied. The results show that the DFT calculation with the hybrid functional is more appropriate. Based on the optimized geometry, we calculate the adsorption energies and the NPA charges. The calculations show that the adsorption energies of CH_3 on the clusters exhibit odd/even alternation with increasing cluster size, but no odd/even alternation for CH_2 case. The obtained adsorption energies for CH_2 are larger than those for CH_3, implying stronger adsorption for CH_2 adsorbed on Cu clusters than for CH_3. The NPA calculations show that the charges transfer from Cu to CH_2 or CH_3, and more charges are transferred to CH_2 than to CH_3. The calculated vibrational frequencies for different modes of CH_2 and CH_3 adsorbed on Cu_n clusters agree with the experimental results of their adsorption on Cu (111) surface.

V. ACKNOWLEDGMENTS

This work was supported by the Chinese Academy of Engineering Physics (No.51480030105JW1301) and

DOI:10.1088/1674-0068/21/05/445-450

the National Natural Science Foundation of China (No.10534010, No.10374036, and No.10374037).

[1] A. Goldberg and I. Yarovsky, Phys. Rev. B **75**, 195403 (2007).
[2] K. C. Prince, E. Holub-Krappe, and K. Horn, Phys. Rev. B **32**, 4249 (1985).
[3] Y. Li, J. M. Hu, and J. Q. Li, Chin. J. Struct. Chem. **23**, 387 (2005).
[4] F. M. Poveda, M. Sánchez, and F. Ruette, J. Phys.: Condens. Matter **5**, A237 (1993).
[5] X. L. Ding, Z. Y. Li, J. L. Yang, J. G. Hou, and Q. S. Zhu, J. Chem. Phys. **120**, 9594 (2004).
[6] R. S. Zhai, Y. L. Chan, P. Chuang, C. K. Hsu, M. Mukherjee, T. J. Chuang, and R. Klauser, Langmuir **20**, 3623 (2004).
[7] W. W. Pai, Y. L. Chan, S. W. Chang, T. J. Chuang, and C. H. Lin, Jpn. J. Appl. Phys. **45**, 2372 (2006).
[8] Y. L. Chan, P. Chuang, and T. J. Chuang, J. Vac. Sci. Technol. A **16**, 1023 (1998).
[9] G. Radhakrishnan, W. Stenzel, R. Hemmen, H. Conrad, and A. M. Bradshaw, J. Chem. Phys. **95**, 3930 (1991).
[10] Q. Y. Yang, K. J. Maynard, A. D. Johnson, and S. T. Ceyer, J. Chem. Phys. **102**, 7734 (1995).
[11] M. L. Colaianni, P. J. Chen, H. Gutleben, and J. T. Yates, Jr., Chem. Phys. Lett. **191**, 561 (1992).
[12] M. Pascal, C. L. A. Lamont, M. Kittel, J. T. Hoeft , L. Constantb, M. Polcik, A. M. Bradshaw, R. L. Toomes, and D. P. Woodruff, Surf. Sci. **512**, 173 (2002).
[13] J. D. Head and Y. Shi, Int. J. Quantum Chem. **75**, 815 (1999).
[14] K. Burke, J. P. Perdew, and Y. Wang, *Electronic Density Functional Theory: Recent Progress and New Directions*, J. F. Dobson, G. Vignale, and M. P. Das, Ed., New York: Plenum, (1998).
[15] A. Michaelides and P. Hu, J. Chem. Phys. **114**, 2523 (2001).
[16] J. Robinson and D. P. Woodruff, Surf. Sci. **498**, 203 (2002).
[17] B. Hammer, L. B. Hansen, and J. K. Norskov, Phys. Rev. B **59**, 7413 (1999).
[18] M. J. Frisch, G. W. Trucks, H. B. Schlegel, G. E. Scuseria, M. A. Robb, J. R. Cheeseman, J. A. Montgomery, Jr., T. Vreven, K. N. Kudin, J. C. Burant, J. M. Millam, S. S. Iyengar, J. Tomasi, V. Barone, B. Mennucci, M. Cossi, G. Scalmani, N. Rega, G. A. Petersson, H. Nakatsuji, M. Hada, M. Ehara, K. Toyota, R. Fukuda, J. Hasegawa, M. Ishida, T. Nakajima, Y. Honda, O. Kitao, H. Nakai, M. Klene, X. Li, J. E. Knox, H. P. Hratchian, J. B. Cross, C. Adamo, J. Jaramillo, R. Gomperts, R. E. Stratmann, O. Yazyev, A. J. Austin, R. Cammi, C. Pomelli, J. W. Ochterski, P. Y. Ayala, K. Morokuma, G. A. Voth, P. Salvador, J. J. Dannenberg, V. G. Zakrzewski, S. Dapprich, A. D. Daniels, M. C. Strain, Ö. Farkas, D. K. Malick, A. D. Rabuck, K. Raghavachari, J. B. Foresman, J. V. Ortiz, Q. Cui, A. G. Baboul, S. Clifford, J. Cioslowski, B. B. Stefanov, G. Liu, A. Liashenko, P. Piskorz, I. Komaromi, R. L. Martin, D. J. Fox, T. Keith, M. A. Al-Laham, C. Y. Peng, A. Nanayakkara, M. Challacombe, P. M. W. Gill, B. Johnson, W. Chen, M. W. Wong, C. Gonzalez, and J. A. Pople, *Gaussian* 03 (*Revision-D*.01), Pittsburgh, PA: Gaussian, Inc., (2003).
[19] J. P. Perdew, J. A. Chevary, S. H. Vosko, K. A. Jackson, M. R. Pederson, D. J. Singh, and C. Fiolhais, Phys. Rev. B **46**, 6671 (1992).
[20] (a) A. D. Becke, J. Chem. Phys. **98**, 5648 (1993).
(b) C. Lee, W. Yang, and R. G. Parr, Phys. Rev. B **37**, 785 (1988).
(c) B. Miehlich, A. Savin, H. Stoll, and H. Preuss, Chem. Phys. Lett. **157**, 200 (1989).
(d) S. H. Vosko, L. Wilk, and M. Nusair, Can. J. Phys. **58**, 1200 (1980).
[21] (a) P. J. Hay and W. R. Wadt, J. Chem. Phys. **82**, 270 (1985).
(b) P. Schwerdtfeger, M. Dolg, W. H. E. Schwarz, G. A. Bowmaker, and P. D. W. Boyd, J. Chem. Phys. **91**, 1762 (1989).
(c) T. V. Russo, R. L. Martin, and P. J. Hay, J. Chem. Phys. **99**, 17085 (1995).
(d) W. C. Eemler, R. B. Ross, and P. A. Christiansen, Int. J. Quantun Chem. **40**, 829 (1991).
[22] S. F. Boys and F. Bernadi, Mol. Phys. **10**, 553 (1970).
[23] S. Simon, M. Duran, and J. J. Dannenberg, J. Chem. Phys. **105**, 11024 (1996).
[24] P. Calaminici, A. M. Köster, A. Vela, and K. Jug, J. Phys. Chem. **113**, 2199 (2000).
[25] D. Post and E. J. Baerends, J. Chem. Phys. **78**, 5663 (1983).
[26] G. Psofogiannakis, A. St-Amant, and M. Ternan, J. Phys. Chem. B **110**, 24593 (2006).
[27] M. K. Oudenhuijzen, J. A. van Bokhoven, D. E. Ramaker, and D. C. Koningsberger, J. Phys. Chem. B **108**, 20247 (2004).
[28] D. R. Alfonso, Sang H. Yang, and D. A. Drabold, Phys. Rev. B **50**, 15369 (1994).
[29] M. R. Pederson, K. A. Jackson, and W. E. Pickett, Phys. Rev. B **44**, 3891 (1991).
[30] K. Larsson, S. Lunell, and J. O. Carlsson, Phys. Rev. B **48**, 2666 (1993).
[31] E. D. Glendening, A. E. Reed, J. E. Carpenter, and F. Weinhold, NBO Version 3.1, Theoretical Chemistry Institute, University of Wisconsin-Madison, (1995).
[32] A. E. Reed, L. A. Cureiss, and F. Wenhold, Chem. Rev. **88**, 899 (1988).
[33] A. P. Scott and L. Radom, J. Phys. Chem. **100**, 16502 (1996).
[34] M. A. Henderson, P. L. Radloff, and J. M. White, J. Phys. Chem. **92**, 4111 (1988).
[35] Y. C. Ning, *Structural Identification of Organic Compounds and Organic Spectroscopy,* 2nd Ed., Beijing: Science Press, (2000).
[36] M. Witko, K. Hermann, D. Ricken, W. Stenzel, H. Conrad, and A. M. Bradshaw, Chem. Phys. **177**, 363 (1993).
[37] (a) G. D. Stancu and J. Röpcke, J. Chem. Phys. **122**, 014306 (2005).
(b) P. L. Holt, K. E. McCurdy, R. B. Weisman, J. S. Adams, P. S. Engel, J. Chem. Phys. **81**, 3349 (1984).
(c) T. Momose, M. Miki, M. Uchida, T. Shimizu, I. Yoshizawa, and T. Shida, J. Chem. Phys. **103**, 1400 (1995).
(d) J. J. Scherer, K. W. Aniolek, N. P. Cernansky, and D. J. Rakestraw, J. Chem. Phys. **107**, 6196 (1997).

DOI:10.1088/1674-0068/21/05/445-450